BJPS

Brazilian Journal of
Pharmaceutical Sciences

http://dx.doi.org/10.1590/s2175-97902022e19859

Article

Development of monolithic matrix type transdermal patches containing cinnarizine: Physical characterization and permeation studies

Şükran Damgalı[1], Samet Özdemir[2], Gizem Kaya[1], Aslı Barla Demirkoz[3,4], Melike Üner[1*]

[1]Istanbul University, Faculty of Pharmacy, Department of Pharmaceutical Technology, Beyazit 34116 Istanbul, Turkey, [2]Istanbul Health and Technology University, Faculty of Pharmacy, Department of Pharmaceutical Technology, Zeytinburnu 34015, Istanbul, Turkey, [3]Aromsa Besin Aroma ve Katkı Maddeleri Sanayi ve Ticaret Anonim Şirketi, Gebze, Kocaeli [4]1480, Turkey, 4Halic University, School of Health Sciences, Department of Nutrition and Dietetics, Beyoglu 34445 Istanbul, Turkey

To overcome the problems associated with bioavailability and systemic side effects of the drug by oral administration, monolithic matrix type transdermal patches containing cinnarizine (CNZ) were developed. For this purpose, films based on hydroxypropyl methylcellulose and polyvinylpyrrolidone as matrix-forming polymers were designed. Physical characteristics of transdermal films and drug-excipient compatibility were investigated. Factors affecting *in vitro* drug release and *ex vivo* skin penetration and permeation of the drug were studied. It was confirmed that films displayed sufficient flexibility and mechanical strength for application onto the skin for a long time period. *Ex vivo* penetration experiments gave satisfactory results for transdermal drug delivery through rat skin. The parameters determining good skin penetration were also evaluated. The highest drug permeation rate was obtained with incorporation of Transcutol® (0.102 mg/cm^2/h) into the base CNZ formulation, followed by propylene glycol (0.063 mg/cm^2/h), menthol (0.045 mg/cm^2/h), and glycerin (0.021 mg/cm^2/h) as penetration enhancers ($p < 0.05$). As a result, the developed transdermal patches of CNZ may introduce an alternative treatment for various conditions and diseases such as idiopathic urticarial vasculitis, Ménière's disease, motion sickness, nausea, and vertigo. Thus, the risk of systemic side effects caused by the drug can be reduced or eliminated.

Keywords: Cinnarizine. Penetration enhancers. Topical application. Transdermal delivery. Transdermal patches.

INTRODUCTION

Cinnarizine (CNZ) is a histamine H1-antagonist and selective calcium channel blocker agent (Sweetman, 2009). Similar to other antihistamines, CNZ possesses anticholinergic and local anesthetic effects. CNZ is used for treatment of a broad variety of conditions and diseases, such as epilepsy, nausea, motion sickness, chemotherapy, vertigo, and Ménière's disease (Djelilovic-Vranic *et al*., 2012). It can be used in cases of post-trauma cerebral symptoms, cerebral apoplexy, and cerebral arteriosclerosis since it promotes cerebral blood flow (Shi *et al*., 2009). CNZ was found to be effective in the treatment of idiopathic urticarial vasculitis (Tosoni *et al*., 2009). It is a weak base and its dissolution behavior is pH-dependent. Its aqueous solubility gradually decreases at pH values above 4. It can easily dissolve at pH 1 (Shi *et al*., 2009). Bioavailability of orally administered CNZ is typically low and variable due to its pH-dependent solubility and high incidence of degradation. Its solutions in water have poor chemical stability at pH 1.2-3.0. The oral bioavailability of CNZ has been shown to depend on its amount of dissolution in the stomach (Ogata *et al*., 1986). Its octanol/water partition coefficient (Log *P*) was reported as 6.14 (Martinez *et al*., 2007).

***Correspondence:** M. Üner. Department of Pharmaceutical Technology. Faculty of Pharmacy. Istanbul University. Beyazit 34116 Istanbul, Turkey. Phone: +90 2124400000. Fax: +90 2124400252. http://orcid.org/0000-0003-2786-5947. E-mail: melikeuner@yahoo.com

CNZ exhibits side effects from mild to quite severe when it is administered orally. The most common side effects of CNZ are gastrointestinal irritation, dry mouth, lethargy, headache, skin problems, hypersensitivity reactions, sweating, muscle rigidity, and tremor (Holmes *et al*., 1984). It can readily pass through the blood-brain barrier and it displays sedative activity, causing drowsiness and blurred vision. Due to the increase in drowsiness levels caused by CNZ, its use by pilots and air crews is often limited (Powell-Dunford and Bushby, 2017).

Topical dosage forms of drugs are often designed to reduce their systemic side effects following oral administration. Skin application of active ingredients might be preferred over their oral application. After oral administration, many drugs are exposed to the first-pass metabolism. The liver is generally considered the primary site of the first-pass metabolism of orally administered drugs. In the first-pass metabolism, the drug is absorbed from the gastrointestinal tract and transported through the portal vein to the liver. It is then metabolized or only a small proportion of it can reach the blood stream. The first-pass metabolism is important particularly for drugs with low or variable oral bioavailability (Pond and Tozer, 1984). In addition, the gastrointestinal tract is one of the other potential sites of first-pass metabolism. The extent of the first-pass metabolism in the liver and intestinal walls depends on a number of physiological factors like plasma protein and blood cell binding, enzyme activity, and gastrointestinal motility. The transdermal route might be an alternative to oral drug administration because it allows the first-pass effect to be avoided (Paudel *et al*., 2010). As an alternative tTo its oral administration, we attempted to optimize transdermal patches of CNZ to avoid the first-pass metabolism, provide an effective therapy, and minimize/eliminate systemic side effects of the drug. For this purpose, transdermal base films and films containing various penetration enhancers were prepared. Films were confirmed to be of the expected pharmaceutical quality by physical characterization tests. Transdermal patches were then produced and *ex vivo* experiments were performed. Effects of penetration enhancers on permeation of CNZ through the skin were investigated.

MATERIAL AND METHODS

Material

Cinnarizine (CNZ) was kindly provided by Nobel İlaç San. ve Tic. A.S. (Turkey). Hydroxypropyl methylcellulose (Methocel K15M) (HPMC) was kindly provided by Colorcon (Turkey). Polyvinylpyrrolidone (PVP-K90) and menthol (M) were purchased from Doğa İlaç Hammaddeler Tic. Ltd. Şti. (Turkey); propylene glycol (PG), polyethylene glycol (PEG 400), and glycerin (Gl) from Merck (Germany); and Transcutol® (Tc) from Gattefosse (France). 3M 9773 foam tape, CoTran 9719 backing, and Scotchpak 1020 release liner for preparing transdermal patches of films were kind gifts from 3M Drug Delivery Systems (Germany). All other chemicals used were of analytical grade.

Determination of partition coefficient of CNZ

Isopropyl myristate and water were reciprocally saturated in a shaking water bath (Daihan Scientific, Korea) at 100 rpm and 25 ± 1 °C for 24 h. Four stock solutions of CNZ in isopropyl myristate (1 mg/mL) were prepared and they were presaturated with water under the same conditions. Supernatants were collected and they were mixed with presaturated isopropyl myristate at ratios of 1:1, 1:3, and 3:1 (v/v). Mixtures were kept in the shaking water bath at 100 rpm and 25 ± 1 °C for 48 h. After centrifugation of mixtures at 6000 rpm for 15 min, the CNZ amount was determined in each phase by high-performance liquid chromatography (HPLC). This process was triplicated for each stock solution (European Chemical Bureau, 1992; Nicoli *et al*., 2008).

Preparation of films and transdermal patches

HPMC, PVP-K90, and various penetration enhancers were used for preparation of placebo and CNZ films (Table I) (Damgalı, 2017). For preparation of the placebo base film formulation (Pl. F-base), a hydrogel containing both HPMC and PVP-K90 in water was prepared. PEG 400 as a plasticizer agent and normal saline (NS) were then added under stirring using an HS-100D propeller mixer (Daihan Scientific, Korea) at 400 rpm for 1 min. The mixture

was then kept in an ultrasonic bath (Bersonic, Turkey) to remove air bubbles for 1 min. It was homogeneously poured into petri dishes of 9 cm in diameter. Petri dishes were kept in the WiseVen Fuzzy Control System (Daihan Scientific, Korea) at 40 ± 2 °C for 48 h. After this drying step, formed films were removed from dishes.

Penetration enhancers were added to Pl. F-base for preparing other placebo formulations (Pl. F-Tc, Pl. F-PG, Pl. F-Gl, and Pl. F-M). The same procedure was used for obtaining films.

For preparation of CNZ transdermal films (F-base, F-Tc, F-PG, F-Gl, and F-M), CNZ was suspended in NS and the 11.11% CNZ suspension was then added to the hydrogel under stirring and the same procedure was followed.

CNZ films were cut to a surface area size of 3.15 cm^2. Monolithic matrix type transdermal patches were then produced by using transdermal patch components (foam tape, backing film, CNZ films, and release liner, respectively) (Figure 1).

TABLE I - Constituents (%) of placebo and CNZ transdermal films

Formulations	Constituents (%)									
	CNZ	HPMC	PVP-K90	PEG 400	NS	Tc	PG	Gl	M	Water
Pl. F-base	-	3.15	0.35	15	22.5	-	-	-	-	56.5
Pl. F-Tc	-	3.15	0.35	15	22.5	5	-	-	-	51.5
Pl. F-PG	-	3.15	0.35	15	22.5	-	5	-	-	51.5
Pl. F-Gl	-	3.15	0.35	15	22.5	-	-	5	-	51.5
Pl. F-M	-	3.15	0.35	15	22.5	-	-	-	2	54.5
F-base	2.5	3.15	0.35	15	22.5	-	-	-	-	56.5
F-Tc	2.5	3.15	0.35	15	22.5	5	-	-	-	51.5
F-PG	2.5	3.15	0.35	15	22.5	-	5	-	-	51.5
F-Gl	2.5	3.15	0.35	15	22.5	-	-	5	-	51.5
F-M	2.5	3.15	0.35	15	22.5	-	-	-	2	54.5

Pl., placebo; NS, normal saline.

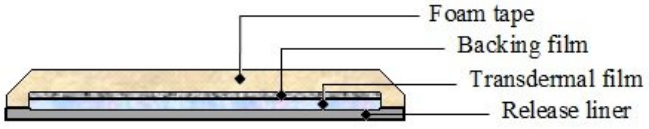

FIGURE 1 - Components of monolithic matrix type transdermal patches containing CNZ.

Determination of weight variation, thickness, and tensile strength of films

Ten circular film pieces of 1 cm in diameter were cut. They were precisely weighed and their thickness was determined using a micrometer (Mitutoyo, Japan).

Tensile strength of film strips cut in the dimensions of 80 mm × 25 mm was determined using a TA-TX Plus Texture Analysis Apparatus (UK). The apparatus was equipped with a TA-DGF dual grip fixture with 25-mm-wide grips fitted with rubber inserts to maximize contact adhesion with sample films (Thakur, Singh, and Singh, 2016). Films were clamped at both ends with grippers and thumbscrews for precise alignment. They were pulled by the upper clamp at a rate of 1 mm/s and with a rotation of 4.5 mm/s. Trigger load was 0.01 N. When films broke, peak load and deformation at peak load were measured. Tensile strength and extensibility of transdermal films were calculated. This study was replicated three times for each formulation.

Fourier transform infrared spectroscopy (FT-IR) analysis

FT-IR analysis was performed to evaluate the interaction between drug and transdermal film excipients (Jatav *et al*., 2013; Akram *et al*., 2018). For this purpose, pure drug (CNZ), placebo, and drug-containing films were scanned in the wave number range of 4000-650 cm^{-1} at resolution of 4 cm^{-1} in a PerkinElmer 100 FT-IR instrument (UK). The apparatus was equipped with PerkinElmer Spectrum Version 6.0.2 Software. Samples were placed on the sample stage and force of 100 N was applied to scan the transmission mode of the instrument.

Differential scanning calorimetry (DSC) analysis

Drug-excipient compatibility was investigated by DSC. DSC analysis was performed on the pure drug and films to investigate possible interactions between the drug and film ingredients (Jatav *et al*., 2013; Akram *et al*., 2018). Samples of 10-12 mg were precisely weighed into standard Tzero™ aluminum hermetic pans of a Universal V4.5A DSC apparatus (TA Instruments/DSC Q2000, USA). Pans were heated from 10 °C to 200 °C with a heating rate of 5 K/min and flushing with 50 mL N_2/min. Melting peaks and enthalpies of samples were calculated using the apparatus software. Crystallization behavior of the drug in transdermal films was investigated.

Quantification of CNZ

HPLC for quantification of CNZ was verified according to the instructions of the ICH Q2 (R1) guidelines for the method validation procedure. For this purpose, specificity, linearity, detection range, accuracy, recovery, intra-day and inter-day precision, and detection/quantification limits of the analytical method were determined. Each verification analysis was replicated six times.

The HPLC apparatus (Shimadzu LC-20AT, Japan) was equipped with a UV/VIS detector (Shimadzu SPD-20A) and SIL-20A HT autosampler (Shimadzu SIL-20A). A TC-C18 column (5 µm, 4.6 × 250 mm) (Agilent Tech, Germany) was used for detection. Injection volume of samples was 20 µL. The mobile phase was acetonitrile:pH 4.5 ammonium phosphate monobasic solution (6:4, v/v). Samples were detected under a mobile phase flow rate of 1 mL/min at 253 nm at 40 °C. Drug determination was carried out at six concentrations (4-24 µg/mL) for providing the calibration curve.

Determination of drug content and content uniformity of films

Circular pieces of 1 cm in diameter cut from films were dissolved in 20 mL of methanol in an ultrasonic bath for 20 min (Damgalı, 2017). Dispersions were filtered through S&S[5893] blue ribbon filter papers (2 µm pore size, Schleicher & Schuell, Germany) and samples of 0.2 mL were taken from supernatants. Samples were diluted with the mobile phase to 10 mL. The CNZ amount in films was assayed by HPLC. This study was replicated three times.

In vitro drug release from transdermal patches

Nitrocellulose membranes (0.45 µm pore size, Millipore, USA) were used between two halves of Franz-type diffusion cells (Çalışkan Cam Teknik, Turkey) with surface area of 3.15 cm^2. Receptor chambers of the cells (33.2 mL) were filled with physiological saline solution:PEG 400 mixture (PSS:PEG 400) (6:4, v/v) (Ham *et al*., 2013). Before the test, membranes were kept in the release medium overnight. Transdermal patches were fixed on nitrocellulose membranes between donor and receptor chambers of the cells. The assembly was set on an SMHS WiseStir magnetic stirrer with 6 points (Witeg Labortechnik GmbH, Germany). Testing was conducted at 37 ± 0.5 °C. One milliliter of sample was taken from each cell at certain time intervals. Release of CNZ was determined by HPLC after appropriate dilution of samples. Six replicates were conducted for each formulation. Drug release profiles were obtained by plotting cumulative amounts of the drug as a function of time. Release profiles were evaluated using different kinetic models (zero-order, first-order, and Higuchi square-root model) (Higuchi, 1963; Korsmeyer *et al*., 1983). The exponent value (n) of the Korsmeyer-Peppas kinetic model was considered for specifying drug release mechanisms.

Ex vivo skin penetration and permeation study

Penetration and permeation properties of the drug through the skin and the effects of penetration enhancers were investigated on experimental animals. For this purpose, the abdominal skins of male Wistar albino rats (200-250 g) were used as the skin model, as reported in earlier studies (Liu *et al*., 2013; Yi *et al*., 2016; Fahmy *et al*., 2018). The experimental protocol was approved by the Local Ethical Committee of Animal Experiments (17.12.2013, No: 2013/131). Rats were housed in plastic cages at 22 ± 1 °C and 60 ± 1% humidity under a 12-h light/dark cycle. They were given the standard laboratory diet and tap water *ad libitum*. For *ex vivo* skin penetration and permeability assessments, carefully shaved full-thickness abdominal skins were obtained after the animals were sacrificed. The underlying fatty tissues of skins were removed by blunt dissection. They were placed between two halves of Franz-type diffusion cells containing PSS:PEG 400 (6:4, v/v) in the receptor phase. Transdermal patches were applied to the surface of rat skins. Penetration of CNZ was assayed by HPLC on samples collected at certain time intervals for 6 hours. The study was conducted at 37 ± 1 °C. The cumulative amount (Q_n, µg/cm^2) of permeated CNZ was determined (Sloan *et al*., 1986; Williams and Barry, 2004; Haq and Michniak-Kohn, 2018). The steady-state flux of the drug (J_s, µg/cm^2/h) was ascertained from the slope of the linear part of the plot using linear regression analysis ($r > 0.99$). Three replicates were conducted for each formulation. Thus, the efficacy of penetration enhancers was determined.

In the next stage, rat skins were taken from Franz-type diffusion cells. They were carefully expunged using cotton swabs in order to remove possible formulation residues in contact with the stratum corneum (Houston *et al*., 2017). Disc-shaped PVC adhesive tape pieces (Vege®, İzmir, Turkey) were provided in 1-cm semidiameter. Adhesive tapes were applied to the diffusion area on skins with light pressure. They were removed with forceps. The first 2 strips were thrown away since they collected the residue of the formulations within the crevices of the skin surface. The next 10 adhesive tapes were applied with hard pressure and then removed with uniform force rapidly using forceps. All adhesive tapes were collected in a 25-mL flask for extracting the drug content. For extraction of CNZ, 10 mL of ethanol was added to each flask and all flasks were tightly closed. They were fixed in a water bath at 25 ± 1 °C. The apparatus was adjusted to 160 rpm continuous agitation for 24 h. Contents of flasks were then filtered through S&S[5893] blue ribbon papers. The amount of CNZ in clear supernatants was determined by HPLC. This study was replicated three times for each formulation.

Data treatment and statistics

Statistical analysis of the data was performed using one-way analysis of variance (ANOVA) and subsequent Tukey post hoc pairwise tests to determine differences. For this purpose, Minitab® 18 Statistical Software was used by setting the level of significance to $\alpha = 0.05$.

RESULTS AND DISCUSSION

Weight variation, film thickness, content uniformity, and tensile strength of films

Physical experiments showed us that the transdermal films were of pharmaceutical quality. All data were obtained with acceptable standard deviations (Table II). Standard deviations from mean CNZ content were found as 0.07%-0.31% (relative standard deviations of data were lower than 1%). Content uniformity of transdermal films was affirmed according to compendial methods (30(4) Harmonization: <905> Uniformity of Dosage Forms, 2016), whereby dosage units and their drug contents are expected to be in the range of 85% to 115% and the relative standard deviation of 10 dosage units must be less than or equal to 6%.

Deformation at peak load, tensile strength, and extensibility of films gave us information on their flexibility and mechanical strength when they are applied to the skin for a long period of time (Table III). Addition of the drug and penetration enhancers was confirmed to increase the extensibility (%) of transdermal films under the load. Tc and PG provided the highest extensibility enhancement (F-Tc and F-PG, $p > 0.05$), followed by M (F-M) and Gl (F-Gl) ($p < 0.05$). This can be attributed to the fact that Tc and PG also displayed the plasticizer function more highly compared to Gl (Rowe, Sheskey, Owen, 2009; El Nabarawi *et al*., 2013).

TABLE II - Weight, thickness and drug content of CNZ transdermal films

Formulations	Weight (mg)	Thickness (mm)	Drug content (mg/cm²)
Pl. F-base	61.13 ± 0.41	0.68 ± 0.01	na
F-base	61.21 ± 0.31	0.69 ± 0.01	7.03 ± 0.31
Pl. F-Tc	62.86 ± 0.19	0.86 ± 0.01	na
F-Tc	64.38 ±0.64	0.87 ± 0.02	6.83 ± 0.12
Pl. F-PG	60.88 ± 0.08	0.59 ± 0	na
F-PG	60.66 ± 0.57	0.59 ± 0.02	6.65 ± 0.09
Pl. F-Gl	72.51 ± 0.42	0.76 ± 0	na
F-Gl	78.09 ± 0.36	0.76 ± 0.01	7.11 ± 0.66
Pl. F-M	72.22 ± 0.32	0.75 ± 0.01	na
F-M	62.59 ± 0.39	0.67 ± 0.01	6.74 ± 0.07

TABLE III - Peak load, deformation at peak load, tensile strength and extensibility of placebo films and CNZ transdermal films

Formulations	PL (N)	DPl (mm)	CSAs	Ts (N/mm²)	E (%)
Pl. F-base	33.28 ± 3.66	41.16 ± 3.12	17.00 ± 0.25	1.96 ± 0.22	51.49 ± 3.90
Pl. F-Tc	27.92 ± 2.71	28.28 ± 4.76	21.50 ± 0.25	1.30 ± 0.24	35.35 ± 5.95
Pl. F-PG	10.14 ± 0.37	35.72 ± 1.40	14.75 ± 0	0.69 ± 0.03	44.65 ± 1.75
Pl. F-Gl	20.88 ± 2.04	32.53 ± 3.57	19.00 ± 0	1.10 ± 0	40.66 ± 4.46
Pl. F-M	31.32 ± 8.81	35.16 ± 2.54	18.75 ± 0.25	1.67 ± 0.47	43.95 ± 3.18

(continues on the next page...)

TABLE III - Peak load, deformation at peak load, tensile strength and extensibility of placebo films and CNZ transdermal films

Formulations	PL (N)	DPl (mm)	CSAs	Ts (N/mm^2)	E (%)
F-base	31.97 ± 2.29	49.40 ± 2.62	17.25 ± 0.25	1.85 ± 0.13	61.75 ± 3.28
F-Tc	30.81 ± 3.28	73.94 ± 5.85	21.75 ± 0.50	1.11 ± 0.15	92.43 ± 7.31
F-PG	30.90 ± 5.62	68.19 ± 6.68	14.75 ± 0.50	2.09 ± 0.38	85.24 ± 8.35
F-Gl	16.58 ± 2.32	39.77 ± 6.28	19.00 ±0.25	0.87 ± 0.12	49.71 ± 7.85
F-M	28.43 ± 0.68	53.54 ± 7.74	16.75 ± 0.25	1.70 ± 0.04	66.93 ± 9.68
Equations	Ts = PL / CSAs			E = (DPI / Li) x 100	

PL: Peak load, DPl: Deformation at peak load, Ts: Tensile strength, E: Extensibility, CSAs: Cross sectional area of sample (mm^2)  , Li: Initial length (80 mm).

FT-IR analysis

FT-IR spectroscopy gave us information to understand whether the interaction between CNZ and film excipients was physical or not. In FT-IR spectra, vibration properties of chemical functional groups of CNZ and excipients were determined (Jatav *et al*., 2013). Thus, it was confirmed that the interaction between the drug and excipients was physical (Figure 2), because the mixing of components caused changes in peak areas of the drug independent of any chemical interaction. Characteristic bands of pure CNZ were observed at 3000 cm^{-1} (aromatic, alkene, and mono-substituted C-H stretching bands), 2900 cm^{-1} (aliphatic and alkane C-H stretching bands), 1600 cm^{-1} (aromatic C=C stretching band), 1500 cm^{-1} and 1450 cm^{-1} (alkane CH_2 bands), 1150 cm^{-1} (C-N stretching band), and 1000 cm^{-1} and 950 cm^{-1} (out of plane aromatic, alkene =C-H out of plane). It was confirmed that these results were consistent with the results of earlier studies (Haress, 2015). In FT-IR spectra of transdermal films, CNZ peaks in the fingerprint area were seen to get broader due to the existence of film excipients. The C-N stretching band of CNZ at 1150 cm^{-1} was shielded by secondary and tertiary hydroxyls of the penetration enhancers' peaks at 1135.42-1020 cm^{-1} as reported earlier (Yeo *et al*., 2018). The C=C aromatic stretching band of CNZ at 1600 cm^{-1} appeared in the spectra of the formulations except for F-base. This band was identified more clearly in the spectra of F-M and F-Gl.

Broader O-H and C-H stretching bands produced by the polymeric film matrix were observed at 3400-3300 cm^{-1} and 3000-2800 cm^{-1}. R-O-R stretching bands and vibrations produced by HPMC were not observed in the fingerprint area due to hydrophilic and lipophilic residues of PEG, although their presence was known (Loh, Tan, Peh, 2014).

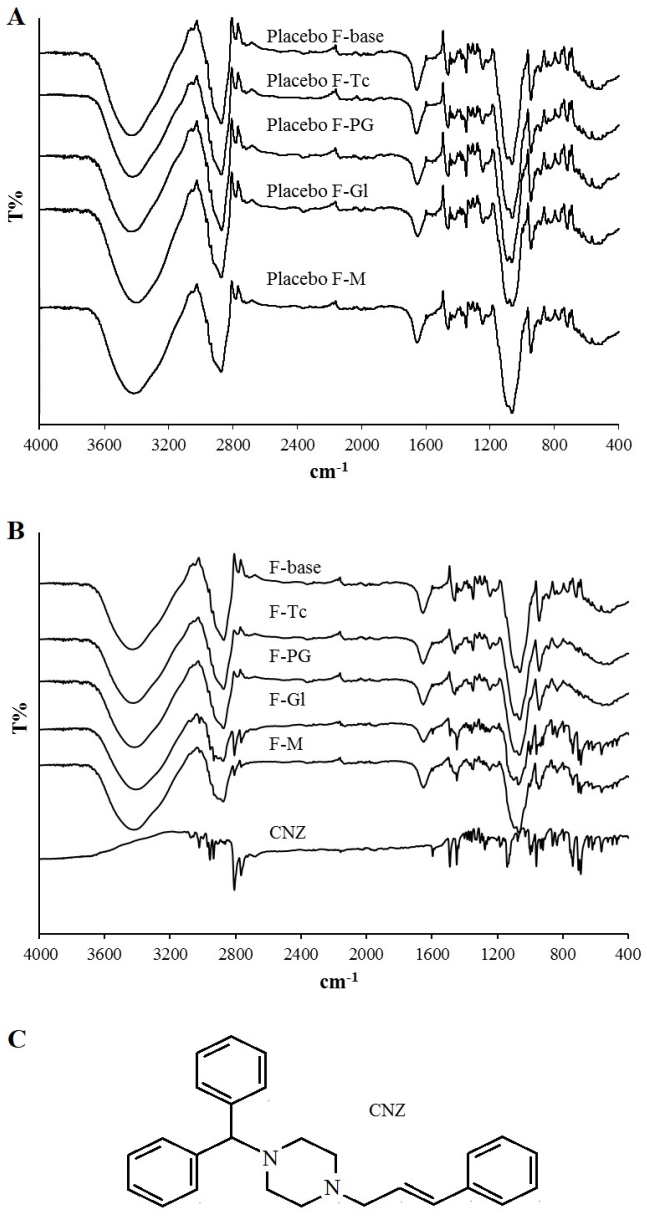

FIGURE 2 - FT-IR profiles of (**A**) placebo film formulations and (**B**) CNZ transdermal films, and (**C**) chemical structure of CNZ [1-(diphenylmethyl)-4-(3-phenyl-2-propenyl)piperazine].

DSC analysis

DSC findings and thermograms were found to support the FT-IR spectroscopy findings (Table IV, Figure 3). In transdermal films, the interaction between the drug and excipients was confirmed to be physical. DSC analysis gave us information about thermal behaviors of CNZ and excipients in transdermal films. On the DSC thermogram of pure CNZ, the drug displayed a sharp endothermic peak at its melting point, 121.94 °C (Thomas, Chong, Chaw, 2013). Theoretical melting enthalpy of CNZ was determined as 98.18 J/g (Kalava, Demirel, Yazan, 2005; Mohamed and Attia, 2017). The crystallinity index was calculated to clarify the crystalline state of CNZ in formulations (Üner and Karaman, 2013). Thus, the crystallographic transition of the drug was demonstrated to be delayed through its incorporation into transdermal films. While the melting point of CNZ decreased to 116.05 °C, its crystallization index in transdermal films was determined to be between 1.09% and 3.09%. PEG 400 as the plasticizer in films was thought to penetrate through clusters of drug crystals and impaired its crystal arrangement. All those findings confirmed the chemical compatibility between the drug and excipients in transdermal films.

TABLE IV - DSC findings of CNZ in transdermal films and pure CNZ

Formulations	MP (°C)	Onset (°C)	ME (J/g)	CI (%)
F-base	117.56	114.60	6.887	2.81
F-Tc	116.36	113.18	6.373	2.60
F-PG	116.76	114.29	2.682	1.09
F-Gl	117.03	114.50	6.870	2.80
F-M	116.05	113.33	7.473	3.05
CNZ	121.94	121.16	98.18	100
Equation	$CI = [ME_{formulation} / (ME_{CNZ} \times C_{CNZ})] \times 100$			

MP: Melting point, ME: Melting enthalpy, CI: Crystallization index, C: Concentration

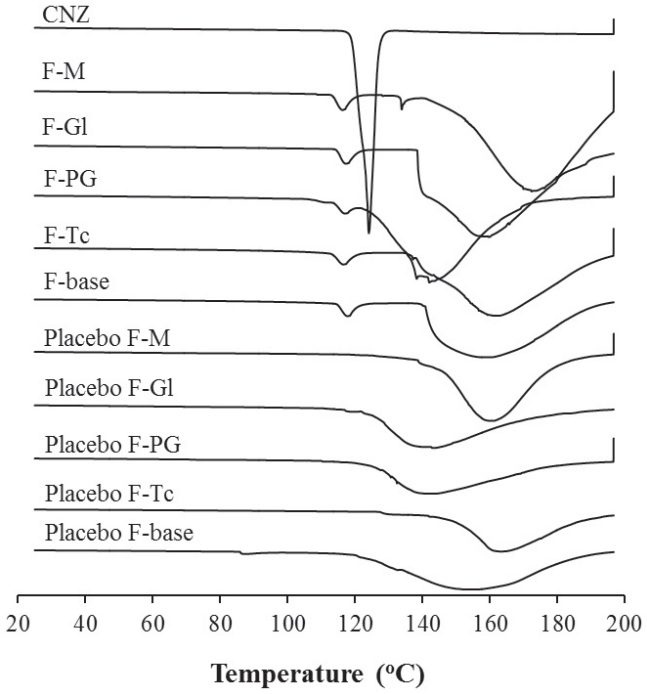

FIGURE 3 - DSC thermograms of CNZ, placebo and CNZ transdermal films.

Quantification of CNZ

Analytical quantification of CNZ by HPLC was verified according to the instructions of the ICH Harmonised Tripartite Guideline (2005). The representative linear equation was A = aC + b, where A is the absorbance, a is the slope, C is the concentration, and b is the intercept. The regression equation was A = 81417.9C + 3405.3 (correlation coefficient: r = 0.9999). The retention time of CNZ was found as 5.8 min. The limit of detection (LOD) and limit of quantification (LOQ) of the quantification method were determined as 5.929 ng/mL and 17.968 ng/mL, respectively. Relative standard deviations for accuracy and intra-day and inter-day precision of the methods were below 2%. Recovery of CNZ was found to range from 99.87 ± 0.06% to 100.74 ± 0.03%. It was confirmed from Figure 4 that the peaks of film ingredients did not interfere with the CNZ peak in the HPLC chromatogram.

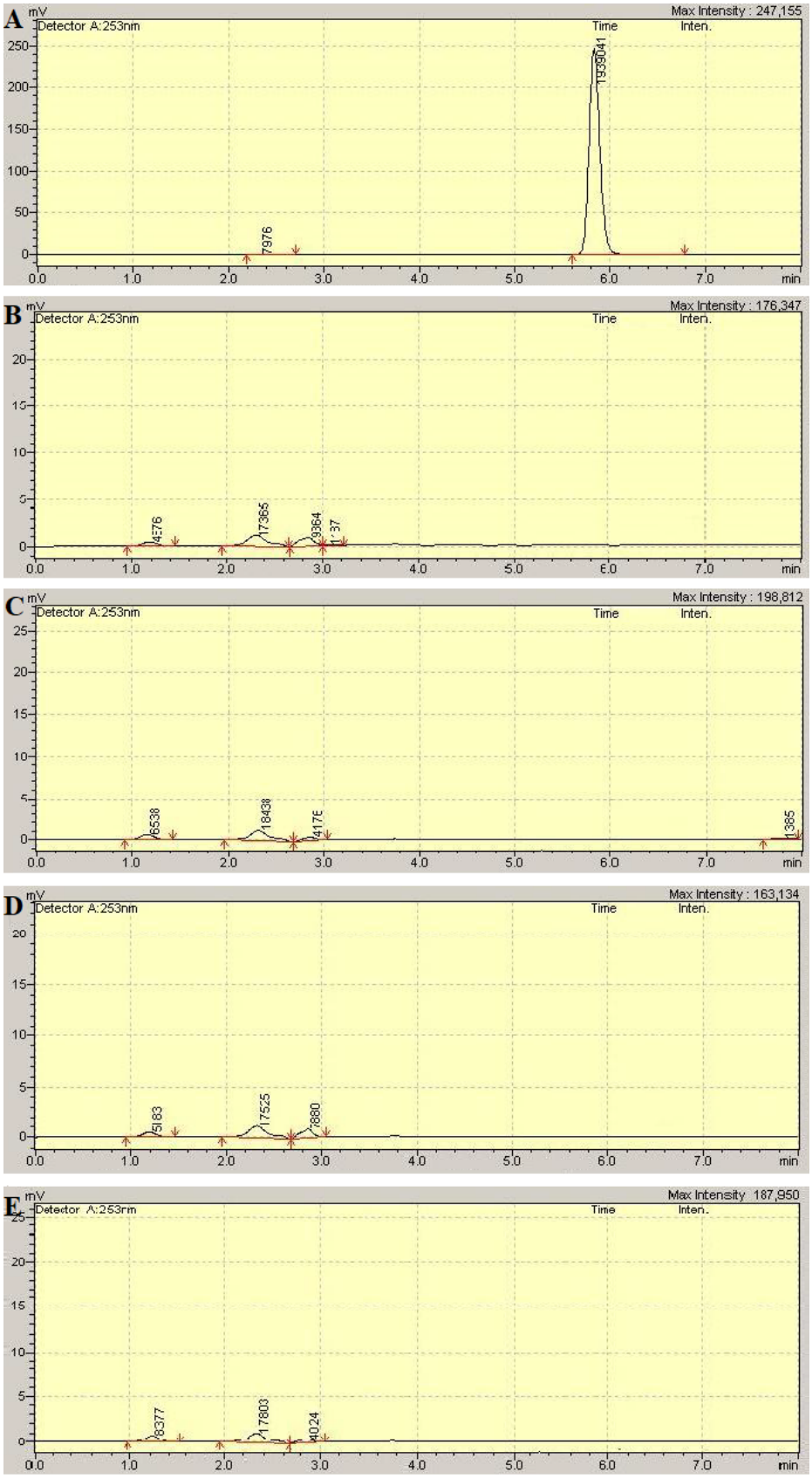

FIGURE 4 – HPLC chromatograms of the drugs and placebo formulations: (**A**) CNZ, (**B**) Pl. F-Tc, (**C**) Pl. F-PG, (**D**) Pl. F-Gl, (**E**) Pl. F-M.

In vitro drug release from transdermal patches

In vitro experiments based on the investigation of release properties of active compounds through synthetic membranes are doubtful for obtaining information about their penetration and permeation properties through the skin. However, these experiments may indicate that the dosage forms are of pharmaceutical quality (Funke *et al*., 2002; Cho *et al*., 2012). At the same time, several researchers showed that the barrier function of synthetic membranes was similar to the barrier function of the stratum corneum. For example, it was reported that the amounts of vitamin D_3 penetrating through a polydimethylsiloxane membrane and through the stratum corneum were very close to each other in *in vitro* and *ex vivo* experiments (Alsaqr, Rasoully, Musteata, 2015). In this study, it was shown that the formulation F-Tc displayed the highest release profile ($p < 0.05$) (Figure 5A). This formulation was followed by formulations F-Gl, F-M, F-PG, and F-base, respectively. Presence of Tc in the film was confirmed to accelerate the drug diffusion rate (1.153 ± 0.008 mg/cm^2/h), probably due to its superior solubilization power compared to many other penetration enhancers as reported earlier (Osborne and Musakhanian, 2018). The difference between the release profiles of formulations F-Gl, F-M, and F-PG was insignificant ($p > 0.05$). Cumulative percentage of drug release versus square root of time curves showed linearity, proving that all formulations followed the Higuchi model and suggesting that diffusion might be the mechanism of drug release (Figure 5B). Correlation coefficients of Higuchi's plot of formulations are presented in Table V. Log cumulative percentage of drug release versus log time curves showed high linearity and proved that all formulations also followed the Korsmeyer-Peppas model. The analysis of regression values of the Higuchi plot and Korsmeyer-Peppas plot and the "n" values of the Korsmeyer-Peppas model showed a combination of diffusional and dissolutional mechanisms, indicating that the drug release from the formulations was controlled by more than one process (Korsmeyer *et al*., 1983). Diffusion exponents of release profiles (slope) from all formulations had values higher than 0.5, indicating a release process controlled by non-Fickian diffusion (Costa and Sousa Lobo, 2003).

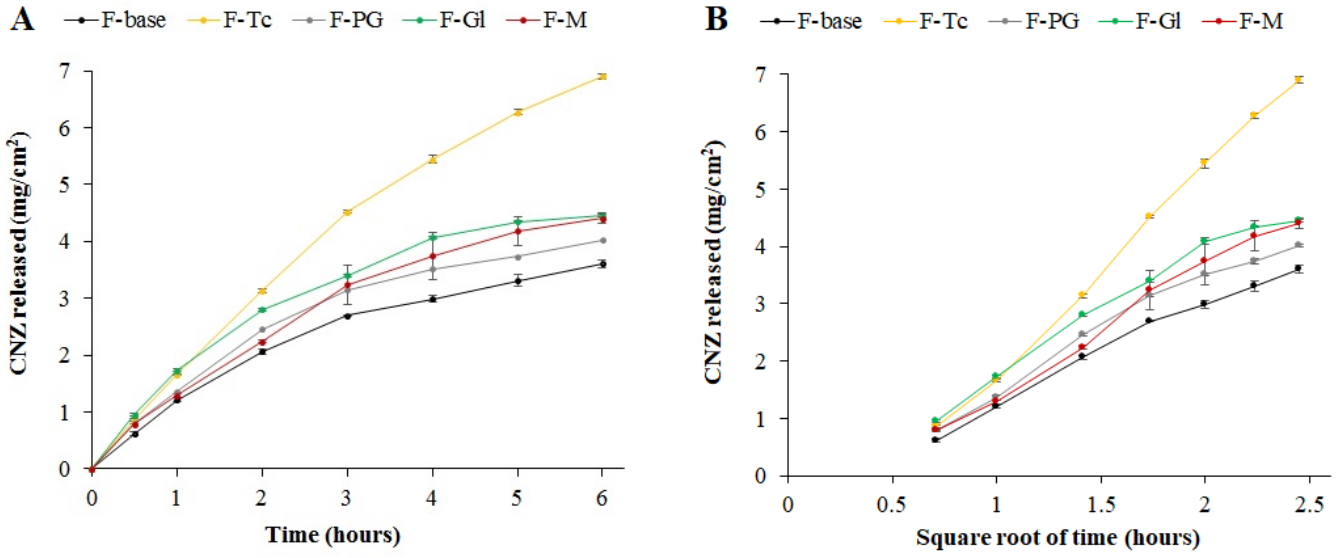

FIGURE 5 - (**A**) Drug release profiles of transdermal patches and (**B**) Higuchi kinetic plots of the drug from formulations.

TABLE V - Release parameters of CNZ from transdermal patches for 6 hours and kinetic modeling of release profiles

Formulations	Q (mg/cm²)	Release rate (mg/cm²/h)	Kinetic models								Dominant release mechanism
			Zero order $[Q_t=Q_0+k_0t]$		First order $[Q_t=Q_\infty(1-e^{-kt})]$		Higuchi model $[Q_t=Q_0+k_H t^{1/2}]$		Korsmeyer-Peppas model $[\log [Q_t/Q_\infty] = \log k + n\log t]$		
			r	k_o	r	k_1	r	D	r	n	
F-base	3.603 ± 0.076	0.602 ± 0.013	0.9671	0.524	0.8947	0.281	**0.9941**	1.719	0.9891	0.70 (non-Fickian)	An.T.
F-Tc	6.906 ± 0.048	1.153 ± 0.008	0.9878	1.113	0.9227	0.349	**0.9988**	3.587	0.9969	0.85 (non-Fickian)	An.T.
F-PG	4.025 ± 0.024	0.672 ± 0.004	0.9559	0.576	0.8940	0.265	**0.9883**	1.900	0.9887	0.66 (non-Fickian)	An.T.
F-Gl	4.450 ± 0.020	0.743 ± 0.004	0.9560	0.632	0.8921	0.251	**0.9886**	2.083	0.9883	0.63 (non-Fickian)	An.T.
F-M	4.406 ± 0.084	0.736 ± 0.014	0.9759	0.679	0.9234	0.296	**0.9948**	2.207	0.9958	0.72 (non-Fickian)	An.T.

Q: cumulative amount of drug released; Q_t *and* Q_0 quantity of drug released at time t and in the release medium at t=0, respectively; r: correlation coefficient; k_1, k_0, and k_H rate constants of the Zero order, First order and Higuchi kinetic models, respectively; Q_t/Q_∞: fractional release of drug; k and n: kinetic constant and diffusion exponent of the release mechanism (slope) according to Korsmeyer-Peppas model; An.T.: Anomalous transport.

Ex vivo skin penetration study drugs

Physicochemical properties of a drug such as molecular mass, melting point, aqueous solubility, and partition coefficient play critical roles in transdermal administration. Drugs with a molecular weight of less than 500 Da, a melting point below 200 °C, and solubility lower than 1 mg/mL can comparatively surpass the barrier function of the stratum corneum. In this case, CNZ with its appropriate molecular weight (368.5 g/mol), melting point (121.94 °C), and low aqueous solubility (1.7 mg/L) can be a candidate molecule for transdermal delivery. On the other hand, as the partition coefficient of a drug increases, its partition into the stratum corneum usually increases. This parameter is especially important when the drug is incorporated into a hydrophilic vehicle (Wiechers, 1989; Ceschel *et al*., 2005). In order to obtain information about the partitioning potential of CNZ into the stratum corneum, the partition coefficient (log *P*) of the drug was determined between isopropyl myristate and water using the shake-flask method. Isopropyl myristate was chosen as the lipophilic phase since its lipophilicity is considered to be similar to that of the stratum corneum (Nicoli *et al*., 2008). The partition coefficient of CNZ was found to be 5.74 ± 0.03. However, the optimum partition coefficient is between 1 and 4 for good drug penetration. In this case, different penetration enhancers were added to the base formulation (F-base) to increase drug penetration through the stratum corneum and the new formulations were evaluated by *ex vivo* experiments. Addition of penetration enhancers was determined to remarkably increase the partition of the drug into the stratum corneum and the flux because the penetration enhancers reduced the barrier resistance of the stratum corneum by different action mechanisms. Presence of Tc in the patch formulation (F-Tc) was affirmed to accelerate the drug permeation rate (0.102 ± 0.003 mg/cm²/h) significantly among other formulations ($p < 0.05$) (Figure 6). Formulations F-PG (0.063 ± 0.002 mg/cm²/h), F-M (0.045 ± 0.0 mg/cm²/h), F-Gl (0.017 ± 0.001 mg/cm²/h), and F-base (0.021 ± 0 mg/cm²/h) followed F-Tc, respectively. Drug permeation was confirmed to reach a steady-state flux at the 30th minute with the highest enhancement ratio (Table VI). Tc is known to not compromise the integrity of the skin structures but to have strong interactions with water of the intercellular path due to its high solubility and solubilization ability (Osborne and Musakhanian, 2018). Strong interaction of Tc with the water of the intercellular path leads to modification of permeation of many drugs through the skin and/or drug retention in the skin. Tc is also known to modify the thermodynamic activity of active compounds in their vehicles after penetrating through tissues themselves at first. Subsequently, active compounds diffuse into

the skin along with modification of driving forces for diffusion (Ganem-Quintanar *et al*., 1997; Osborne and Musakhanian, 2018). PG is also reported to display the same action in addition to its penetration-promoting activity by dissolving α-keratin within the stratum corneum, subsequently reducing the tissue binding of active compounds. Although many researchers reported terpenes to not be as promising penetration enhancers, M was observed to increase drug permeation compared to formulations free of any penetration enhancer (F-base) ($p < 0.05$). The penetration enhancing effect of M can be attributed to its favorable distribution into the intercellular spaces of the stratum corneum and the possible reversible disruption of the intercellular lipid domain (Kunta *et al*., 1997). Gl was determined not to increase CNZ penetration when comparing formulation F-Gl to F-base ($p > 0.05$). The J_s values of the formulations varied (Table VI). Lag time of formulations was determined to be 0.5-1 hours.

TABLE VI - Permeation parameters of CNZ through the skin

Formulations	Q_n (mg/cm^2)	J_s (mg/cm^2/h)	K_p (cm/h)	r	*ER*
F-base	0.132 ± 0.004	0.042 ± 0.005	5.68 x 10^{-3} ± 6.22 x 10^{-4}	0.9923	-
F-Tc	0.869 ± 0.012	0.099 ± 0.001	14.40 x 10^{-3} ± 1.75 x 10^{-4}	0.9974	2.36
F-PG	0.604 ± 0.008	0.044 ± 0.007	6.54 x 10^{-3} ± 10.80 x 10^{-4}	0.9930	1.05
F-Gl	0.156 ± 0.004	0.074 ± 0.003	10.41 x 10^{-3} ± 3.90 x 10^{-4}	0.9946	1.76
F-M	0.487 ± 0.016	0.032 ± 0	4.81 x 10^{-3} ± 0.61 x 10^{-4}	0.9880	0.76

Q_n: cumulative amount of the drug permeated; J_s: steady state flux of the drug; K_p: permeability coefficient; r: correlation coefficient; ER: the enhancement ratio.

In formulation F-Tc, according to the tape stripping test, the amount of CNZ extracted from the stratum corneum was significantly lower than in the receptor phase (Figure 7). The highest difference between the amount of the drug in the stratum corneum and receptor phase was observed with F-Tc, respectively followed by F-PG and F-M, which displayed increased drug permeation. This can be attributed to the high penetration-enhancing activity of Tc through the skin. Glycerin, which is added to topical formulations as a moisturizer, displays a penetration-enhancing effect in combination with water. Thus, glycerin was determined to provide a quite weak penetration-enhancing effect due to removal of almost all of the water during preparation of the transdermal films (F-Gl). The limited water content of the formulation was confirmed to cause greater drug retention in the stratum corneum compared to the base formulation without any penetration enhancer (F-base). However, both of these formulations were insufficient for permeation of CNZ through the skin.

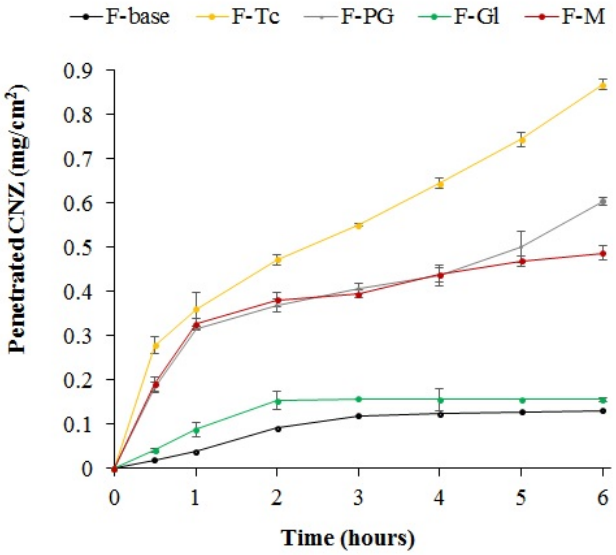

FIGURE 6 - Drug permeation profiles of transdermal patches.

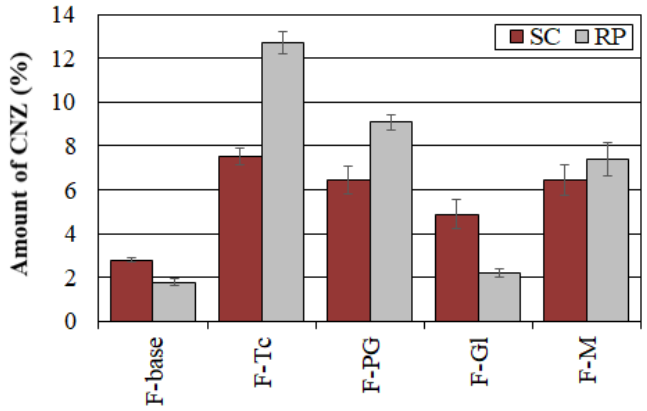

FIGURE 7 - Cumulative amount of CNZ (%) retained in the stratum corneum (SC) of Wistar albino rat skins and remaining in the receptor phase (RP) 6 h after the application of different formulations.

CONCLUSION

Monolithic matrix type transdermal patches of CNZ were successfully optimized in this study. Among various penetration enhancers, Tc resulted in the highest permeation rate of the drug. It was concluded that transdermal patches of CNZ could be used in the treatment of a wide variety of conditions and diseases such as idiopathic urticarial vasculitis, nausea, motion sickness, vertigo, and Ménière's disease. Administration of CNZ with monolithic transdermal patches could be an alternative to oral administration. The dose of the drug can be adjusted by preparing transdermal patches of desired sizes. As an additional advantage, the risk of systemic side effects caused by CNZ can be minimized.

DECLARATION OF INTEREST

The authors report no conflicts of interest. The authors alone are responsible for the content and writing of this article.

ACKNOWLEDGMENTS

This study was supported by the research fund of Istanbul University (Project number: 40188) and TUBITAK (the Scientific and Technological Research Council of Turkey) (Grant Number TEYDEB 1649B031305845).

The authors thank Murat Yasa, Melis Yasa, Mehmet Ak, and İbrahim Gökçe Erdem in AROMSA A.Ş. in Kocaeli, Turkey, for their support in DSC analysis in this study. We also thank Product Executive Asef Özhan in SEM Laboratuvar Cihazları Pazarlama Sanayi ve Ticaret A.Ş. in Istanbul, Turkey, for his support in the tensile strength measurements of transdermal films.

REFERENCES

30(4) Harmonization: <905> Uniformity of Dosage Forms. [citad 2016 Nov 21]. Available from: https://www.usp.org/sites/default/files/usp/document/harmonization/gen-method/q0304_pf_30_4_2004.pdf.

Akram MR, Ahmad M, Abrar A, Sarfraz RM, Mahmood A. Formulation design and development of matrix diffusion controlled transdermal drug delivery of glimepiride. Drug Des Devel Ther. 2018;12:349-64.

Alsaqr A, Rasoully M, Musteata FM. Investigating transdermal delivery of vitamin D3. AAPS PharmSciTech. 2015;16(4):963-72.

Ceschel GC, Bergamante V, Maffei P, Lombardi Borgia S, Calabrese V, Biserni S, et al. Solubility and transdermal permeation properties of a dehydroepiandrosterone cyclodextrin complex from hydrophilic and lipophilic vehicles. Drug Deliv. 2005;12(5):275-80.

Cho CW, Kim DB, Cho HW, Shin SC. Enhanced controlled transdermal delivery of ambroxol from the EVA matrix. Indian J Pharm Sci. 2012;74(2):127-32.

Costa P, Sousa Lobo JM. Evaluation of mathematical models describing drug release from estradiol transdermal systems. Drug Dev Ind Pharm. 2003;29(1):89-97.

Damgalı Ş. Preparation and characterization of cinnarizine topical dosage forms. [Doctoral dissertation]. Istanbul: Istanbul University; 2017.

Djelilovic-Vranic J, Alajbegovic A, Tiric-Campara M, Volic A, Sarajlic Z, Osmanagic E, et al. Betahistine or cinnarizine for treatment of Meniere's disease. Med Arch. 2012;66(6):396-8.

El Nabarawi MA, Shaker D, Attia DA, Hamed SA. In vitro skin permeation and biological evaluation of lornoxicam monolithic transdermal patches. Int J Pharm Pharm Sci. 2013;5(2):242-8.

European Chemical Bureau, Dir 92/69/EEC. [citad 1992 Jul 31]. Available from: https://publications.europa.eu/en/publication-detail/-/publication/17c85561-c516-4dff-aed6-e908140f9bb3.

Fahmy AM, El-Setouhy DA, Ibrahim AB, Habib BA, Tayel SA, Bayoumi NA. Penetration enhancer-containing spanlastics (PECSs) for transdermal delivery of haloperidol: *in vitro* characterization, *ex vivo* permeation and *in vivo* biodistribution studies. Drug Deliv. 2018;25(1):12-22.

Funke AP, Schiller R, Motzkus HW, Günther C, Müller RH, Lipp R. Transdermal delivery of highly lipophilic drugs: in vitro fluxes of antiestrogens, permeation enhancers and solvents from liquid formulations. Pharm Res. 2002;19(5):661-8.

Ganem-Quintanar A, Lafforgue C, Falson-Rieg F, Buri P. Evaluation of the transepidermal permeation of diethylene glycol monoethyl ether and skin water loss. Int J Pharm. 1997;147(2):165-71.

Ham AS, Lustig W, Yang L, Boczar A, Buckheit KW, Buckheit Jr RW. *In vitro* and ex *vivo* evaluations on transdermal delivery of the HIV inhibitor IQP-0410. PLOS One. 2013;8(9):e75306.

Haq A, Michniak-Kohn B. Effects of solvents and penetration enhancers on transdermal delivery of thymoquinone: permeability and skin deposition study. Drug Deliv. 2018;25(1):1943-9.

Haress NG. Cinnarizine: Comprehensive profile. Profiles Drug Subst Excip Relat Methodol. 2015;40:1-41.

Higuchi T. Mechanism of sustained action medication. Theoretical analysis of rate of release of solid drugs dispersed in solid matrices. J Pharm Sci. 1963;52:1145-9.

Holmes B, Brogden RN, Heel RC, Speight TM, Avery GS. Flunarizine. A review of its pharmacodynamic and pharmacokinetic properties and therapeutic use. Drugs. 1984;27(1):6-44.

Houston DMJ, Bugert J, Denyer SP, Heard CM. Anti-inflammatory activity of *Puni*c*a granatum* L. (Pomegranate) rind extracts applied topically to *ex vivo* skin. Eur J Pharm Biopharm. 2017;112:30-7.

ICH Harmonised Tripartite Guideline: Validation of Analytical Procedures: Text and Methodology Q2 (R1). Harmonization Co, Editor; [citad 2005 Nov]. Available from: https://www.ich.org/fileadmin/Public_Web_Site/ICH_Products/Guidelines/Quality/Q2_R1/Step4/Q2_R1__Guideline.pdf.

Jatav VS, Saggu JS, Sharma AK, Sharma A, Jat RK. Design, development and permeation studies of nebivolol hydrochloride from novel matrix type transdermal patches. Adv Biomed Res. 2013;2:62.

Kalava BH, Demirel M, Yazan Y. Physicochemical characterization and dissolution properties of cinnarizine solid dispersions. Turkish J Pharm Sci. 2005;2(2):51-62.

Korsmeyer RW, Gurny R, Doelker E, Buri P, Peppas NA. Mechanisms of solute release from porous hydrophilic polymers. Int J Pharm. 1983;15(1):25-35.

Kunta JR, Goskonda VR, Brotherton HO, Khan MA, Reddy IK. Effect of menthol and related terpenes on the percutaneous absorption of propranolol across excised hairless mouse skin. J Pharm Sci. 1997;86(12):1369-73.

Liu X, Chen T, Liu X, Chen Y, Wang L. Penetration effect of ostrich oil as a promising vehicle on transdermal delivery of sinomenine. J Oleo Sci. 2013;62(9):657-64.

Loh GOK, Tan YT, Peh KK. Effect of HPMC concentration on β-cyclodextrin solubilization of norfloxacin. Carbohydr Polym. 2014;101:505-10.

Martinez MA, Carril-Aviles MM, Sagrado S, Villanueva-Camanas RM, Medina-Hernandez MJ. Characterization of antihistamine-human serum protein interactions by capillary electrophoresis. J Chromatogr A. 2007;1147(2):261-9.

Mohamed MA, Attia AK. Thermal behavior and decomposition kinetics of cinnarizine under isothermal and non-isothermal conditions. J Therm Anal Calorim. 2017;127(2):1751-56.

Nicoli S, Zani F, Bilzi S, Bettini R, Santi P. Association of nicotinamide with parabens: Effect on solubility, partition and transdermal permeation. Eur J Pharm Biopharm. 2008;69(2):613-21.

Ogata H, Aoyagi N, Kaniwa N, Ejima A, Sekine N, Kitamura M, et al. Gastric acidity dependent bioavailability of cinnarizine from two commercial capsules in healthy volunteers. Int J Pharm. 1986;29(1-2):113-20.

Osborne DW, Musakhanian J. Skin penetration and permeation properties of Transcutol® - Neat or diluted mixtures. AAPS PharmSciTech. 2018;19(8):3512-33.

Paudel KS, Milewski M, Swadley CL, Brogden NK, Ghosh P, Stinchcomb AL. Challenges and opportunities in dermal/transdermal delivery. Ther Deliv. 2010;1(1):109-31.

Pond SM, Tozer TN. First-pass elimination. Basic concepts and clinical consequences. Clin Pharmacokinet. 1984;9(1):1-25.

Powell-Dunford N, Bushby A. Management of sea sickness in susceptible flight crews. Mil Med. 2017;182(11):e1846-50.

Rowe RC, Sheskey PJ, Owen SC. Handbook of Pharmaceutical Excipients. 6th ed. New York: Pharmaceutical Press; 2009. p. 624-626.

Shi S, Chen H, Cui Y, Tang X. Formulation, stability and degradation kinetics of intravenous cinnarizine lipid emulsion. Int J Pharm. 2009;373(1-2):147-55.

Sloan KB, Koch SA, Siver KG, Flowers FP. Use of solubility parameters of drug and vehicle to predict flux through skin. J Invest Dermatol. 1986;87(2):244-52.

Sweetman SC. Martindale: The Complete Drug Reference. 36th ed. New York: Pharmaceutical Press; 2009. p. 573-574.

Thakur G, Singh A, Singh I. Formulation and evaluation of transdermal composite films of chitosan-montmorillonite for the delivery of curcumin. Int J Pharm Investig. 2016;6(1):23-31.

Thomas S, Chong YN, Chaw CS. Preparation and characterization of enteric microparticles by coacervation. Drug Dev Ind Pharm. 2013;39(7):1142-51.

Tosoni C, Lodi-Rizzini F, Cinquini M, Pasolini G, Venturini M, Sinico RA, et al. A reassessment of diagnostic criteria and treatment of idiopathic urticarial vasculitis: a retrospective study of 47 patients. Clin Exp Dermatol. 2009;34(2):166-70.

Üner M, Karaman EF. Preliminary studies on solid lipid microparticles of loratadine for the treatment of allergic reactions via the nasal route. Trop J Pharm Res. 2013;12(3):287-93.

Wiechers JW. The barrier function of the skin in relation to percutaneous absorption of drugs. Pharm Weekbl Sci. 1989;11(6):185-98.

Williams AC, Barry BW. Penetration enhancers. Adv Drug Deliv Rev. 2004;56(5):603-18.

Yeo LK, Olusanya TOB, Chaw CS, Elkordy AA. Brief effect of a small hydrophobic drug (cinnarizine) on the physicochemical characterisation of niosomes produced by thin-film hydration and microfluidic methods. Pharmaceutics. 2018;10(4):E185.

Yi QF, Yan J, Tang SY, Huang H, Kang LY. Effect of borneol on the transdermal permeation of drugs with differing lipophilicity and molecular organization of stratum corneum lipids. Drug Dev Ind Pharm. 2016;42(7):1086-93.

Received for publication on 17th September 2019
Accepted for publication on 06th May 2020